Tailored Magnetic Properties of a Double Tetrahedral Molecule with Mixed (1, ½) Spin

Mohamed El Hafidi (mohamed.elhafidi@univh2c.ma)
Hassan II University of Casablanca https://orcid.org/0000-0002-7222-6530
Said Id Bakas
Hassan II University of Casablanca

Research Article

Keywords: Double Tetrahedral molecule, Mixed spin, Magnetization plateaus, Frustration, Quantum Phase Transition, Residual entropy, Magnetocaloric Effect, Giant Spin

Posted Date: May 3rd, 2022

DOI: https://doi.org/10.21203/rs.3.rs-1612314/v1

Tailored Magnetic Properties of a Double Tetrahedral Molecule with Mixed (1, ½) Spin

Said Id Bakas and Mohamed El Hafidi
Laboratory of Condensed Matter Physics
Hassan II University of Casablanca
Faculty of Science Ben M'sik
20630 Casablanca, Morocco

Abstract

In this paper, we study the magnetic properties of a molecule composed of two inverted spin-½ tetrahedra sharing their common vertex via a spin-1. We achieve an exact resolution using the Heisenberg model. As long as the exchange couplings are predominantly ferromagnetic, the spin structure is fully saturated and behaves like a large spin-4 unique magnet.
Antiferromagnetic coupling can strongly frustrate the spins of the nanodevice. This may lead to several exotic phenomena. Therefore, the magnetization can be quantified into plateaus separated by quantum phase transitions.
The work is intended to inspire researchers to develop molecular magnets as a basis for innovative nanoscale engineering applications.

Key-words

Double Tetrahedral molecule, Mixed spin, Magnetization plateaus, Frustration, Quantum Phase Transition, Residual entropy, Magnetocaloric Effect, Giant Spin,

1. Introduction

Modern nanoscale technologies introduced in various areas such as medicine, industry, information storage [1], spintronics [2], superconductivity [3]... are based on the manipulation of atoms, molecules or clusters to create functional components or quantum computer devices [4].
Moreover, these technologies are advantageous on two levels. On the theoretical level, since they can explain certain microscopic physical phenomena such as electrical, thermal conductivity [5, 6], optical properties [7], and even more precisely the magnetic properties of dots (0D) structures [8] on model prototypes. Thus, they open up new possibilities for alternative applications in medicine, information processing, functional devices, etc. Due to rapid technological advancement, the size of electronic and magnetic devices is constantly decreasing. New solutions are required to avoid reaching the size limit of conventional techniques. These challenges spur further research at the nanoscale.

Magnetically, it is now possible to develop single-molecule magnets with controlled moments, including molecules with giant spins in their ground states [6].

As a result of these nanomagnets, a wide variety of potential applications are opened up. For instance, soft magnetic robots are currently being studied deeply for applications beyond the biomedical field, like flexible electronic devices and reconfigurable surfaces, and active metamaterials. Since their discovery, superatoms, supermolecules, and clusters with large quantum spin have attracted both theoretical and experimental research because of their many novel properties [6, 8].

In this paper, we investigate the ferrimagnetic behavior and the frustration phenomena in a double tetrahedral molecule consisting of two tetrahedrons with six identical spin ½ atoms at their basic corners, connected at their common summit corner, by another atom with spin 1. The issue will be addressed in the context of the Heisenberg model with single-ion anisotropy, and will be solved exactly.

The rest of the paper will be structured as follows:

The molecule and the corresponding mixed-spin Heisenberg Hamiltonian will be described in Section 2. We will then diagonalize the Hamiltonian, derive the partition function, and explain the technical details leading to the computation of magnetic and thermodynamic variables. In Section 3, the main results will be exposed and discussed. We will pay special attention to the frustration embedded in this structure, its effects, and consequences. Finally, conclusions and some perspectives will be provided.

2. System Description and Spin Hamiltonian

Consider a molecule made of two identical tetrahedra with equilateral bases connected by the summit. The corner sites of the two base triangles are occupied by atoms or ions with spin-½, such as Cu^{2+}, Ti^{3+} or V^{4+} , while the common summit site between the two tetrahedra is occupied by an atom or ion with spin-1, such as Ni^{2+} , Ti^{2+}or V^{3+} [9]. The three basic spins-½ of each tetrahedron are mutually coupled to each other via exchange, and also to the central spin-1 at the common summit. The core spin-1 is also submitted to the local single-ion anisotropy D , and the whole cluster can be subjected to a magnetic field $\boldsymbol{B}$ parallel to the z-axis of the double tetrahedron (see Figure 1).

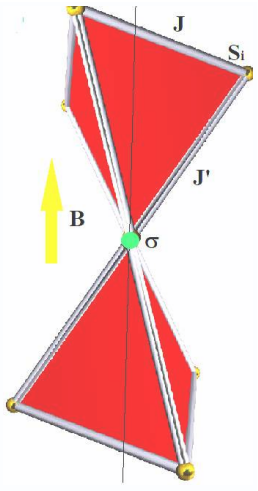

Figure 1 : Illustration of the double tetrahedral molecule. In the basic triangles, the spins-½ $\hat{S}_i$ (i = 1-3) interact with each other through exchange coupling *J*, while the exchange coupling between spins σ and $\hat{S}_i$ (i=1-3) is noted *J'*. The vertical ascending arrow indicates the applied magnetic field.

Our work was inspired by a previous study on an organometallic complex, "Mn_6Cr", which is composed of two trinuclear manganese triplesalen complexes with one $[Cr(CN6)]^{3-}$ ion [10,11].
This molecule is made by six Mn^{3+} ions arranged in two bowl-shaped trinuclear triplesalen building blocks which are linked by a hexacyanochromate. The two tetrahedrons are linked by a block containing an ion Cr^{3+}. In this molecule, the Mn^{3+} and Cr^{3+} ions have respectively a spin 2 and 3/2, strongly coupled antiferromagnetically, leading to a large ground state value of resultant spin 21/2.
In our study, we propose a new molecule which could be synthetized by replacing the Mn^{3+} ion with Ti^{3+} , Cu^{2+}, or V^{4+} (with half-integer spin ½), and the Cr^{3+} ion with V^{3+}, Ni^{2+} or Ti^{2+} (with integer spin 1).

To investigate the magnetism of this mixed-spin molecule, we employ the Heisenberg Hamiltonian with an additional ion-anisotropy term. Therefore, the spin Hamiltonian can be decomposed into three contributions :

$$H = H_{exch} + H_a + H_z \quad (1)$$

where the first, the second, and the third terms denote respectively the exchange, the anisotropy, and Zeeman parts.
Let's now define each term separately:
-the exchange Heisenberg Hamiltonian:

$$H_{exch} = 2H_{ex(S)} + 2H_{ex(\sigma S)} \quad (2)$$

$$H_{ex(S)} = -J(\hat{S}_1.\hat{S}_2 + \hat{S}_1.\hat{S}_3 + \hat{S}_2.\hat{S}_3) = -\frac{J}{2}(\hat{S}^2 - \hat{S}_1^2 - \hat{S}_2^2 - \hat{S}_3^2) \quad (3)$$

where J is the exchange constant coupling the $\hat{S}_i$ spin operators in the top or bottom triangles, and

$$\hat{S} = \hat{S}_1 + \hat{S}_2 + \hat{S}_3 \quad (4)$$

$$H_{ex(\sigma S)} = -J'\hat{\sigma}.\hat{S} = -\frac{J'}{2}(\hat{S'}^2 - \hat{S}^2 - \hat{\sigma}^2) \quad (5)$$

where J' is the exchange constant coupling central spin $\hat{\sigma}$ to the $\hat{S}_i$ (i=1-3) spin operators on the top (or the bottom) triangle, and

$$\hat{S'} = \hat{S} + \hat{\sigma} \quad (6)$$

where $\hat{S}_i = 1/2$ (for i=*1-3*) , and $\sigma = 1$

-the uniaxial anisotropy term :

$$H_a = H_{a(\sigma)} = -D(\sigma^z)^2 \quad (7)$$

It is due to local single-ion anisotropy acting on the spin-1 site, where the anisotropy constant D can be positive or negative. Positive values of D enhance alignment of the spin operator σ along the z-axis, while negative values minimize the z-component, and favorize transverse components in the (x, y) plane. It should be noted that this anisotropy only affects spins larger than ½ .

-the Zeeman term:

$$H_z = 2H_{z(S)} + H_{z(\sigma)} = -2g_S\mu_B BS^z - g_\sigma\mu_B B\sigma^z \quad (8)$$

where : $S^z = S_1^z + S_2^z + S_3^z$, while g_{α} ($\alpha = S, \sigma$), μ_B, and B denote respectively the Landé factor, the Bohr magneton and the applied magnetic field. For simplification, let's take $g_S = g_\sigma = g$, and $h = g\mu_B B$.

In this way, the Hamiltonians H_{exch}, H_a, *and* H_z are diagonalizable and commute between each other, they therefore admit a common system eigenstates noted :

$|\prod_{i=1}^{3} \otimes m_i, m_\sigma, S, S' >$, where $S_i^z|m_i >= m_i|m_i > (m_i = \pm\frac{1}{2}; i = 1, 2, 3)$, and $\sigma^z|m_\sigma >= m_\sigma|m_\sigma > (m_\sigma = \pm 1, 0)$. According to the theorems of angular momentum addition, the quantum numbers S, S', and σ are related by the triangular rule:

$|S - \sigma| \leq S' \leq S + \sigma$

The same rule applies to S, which can have the value ½ or 3/2. Therefore, the eigenenergies of the global Hamiltonian will be:

$$E_{\{m_i\},S,m_\sigma,S'} =$$

$$-J\{S(S+1)-\frac{9}{4}\}-J'\{S'(S'+1)-S(S+1)-\sigma(\sigma+1)\}-Dm_\sigma^2-2hM-h\,m_\sigma \quad (9)$$

where $M=\sum_{i=1}^{3} m_i$. Thus, some eigenenergies are degenerate $G_{SS'}$.

By varying the applied field intensity, the energy levels can be split into sublevels, and the degeneracy can be partially or totally reduced.

The analysis of standard variables requires the computing of the partition function:

$$Z=\sum_{\{\{m_i\},S,m_\sigma,S'\}} G_{SS'} e^{-\beta E(\{m_i\},S,m_\sigma,S')} \quad (10)$$

which can also be written in the following simplified form:

$$Z=A(T,h)+B(T,h)+C(T,h) \quad (11)$$

where

$$A(T,h)=6e^{\frac{-3}{2}\beta J}[e^{\beta D}(ch(2\beta h)+1)+ch(\beta h))(e^{\beta J'}+e^{-2\beta J'})] \quad (12)$$

$$B(T,h)=6e^{\frac{3}{2}\beta J}[e^{\beta D}(ch(2\beta h)+1)+ch(\beta h))(e^{-2\beta J'}+e^{3\beta J'}+e^{-5\beta J'})] \quad (13)$$

$$C(T,h)=2e^{\frac{3}{2}\beta J}[e^{\beta D}(ch(4\beta h)+ch(2\beta h))+ch(\beta h))(e^{-2\beta J'}+e^{3\beta J'})] \quad (14)$$

where $\beta=\frac{1}{k_B T}$, k_B denotes the Boltzmann constant, and T is the absolute temperature.

These preliminary calculations will help us to derive other key variables, such as the magnetization defined by :

$$m=\frac{g\mu_B}{\beta Z}\frac{\partial Z}{\partial h} \quad (15)$$

which can also be written in the simplified form:

$$m=g\mu_B\frac{A'+B'+C'}{Z} \quad (16)$$

where

$$A'=\frac{\partial A}{\beta\partial h}=6e^{\frac{-3}{2}\beta J}[2e^{\beta D}sh(2\beta h)+sh(\beta h))(e^{\beta J'}+e^{-2\beta J'})] \quad (17)$$

$$B'=\frac{\partial B}{\beta\partial h}=6e^{\frac{3}{2}\beta J}[2e^{\beta D}sh(2\beta h)+sh(\beta h))(e^{-2\beta J'}+e^{3\beta J'}+e^{-5\beta J'})] \quad (18)$$

$$C'=\frac{\partial C}{\beta\partial h}=2e^{\frac{3}{2}\beta J}[e^{\beta D}(4sh(4\beta h)+2sh(2\beta h))+sh(\beta h))(e^{-2\beta J'}+e^{3\beta J'})] \quad (19)$$

The initial magnetic susceptibility can also be derived as :

$$\chi=lim_{h\to 0}\left(\frac{\partial m}{\partial h}\right)_h \quad (20)$$

and can be presented in the simplified form

$$\chi(T)=\frac{\chi_0}{k_B T}\frac{A''+B''+C''}{A(T,0)+B(T,0)+C(T,0)} \quad (21)$$

where

$$\chi_0 = (g\mu_B)^2 \quad (22)$$

and

$$A(T,0) = e^{\frac{3}{2}\beta J}[e^{\beta D}+1][e^{-5\beta J'}+e^{-2\beta J'}+e^{3\beta J'}] \quad (29)$$

$$B(T,0) = 3e^{\frac{3}{2}\beta J}[2e^{\beta D}+1][e^{-5\beta J'}+e^{-2\beta J'}+e^{3\beta J'}] \quad (30)$$

$$C(T,0) = 3e^{\frac{3}{2}\beta J}[2e^{\beta D}+1][e^{-5\beta J'}+e^{-2\beta J'}+e^{3\beta J'}] \quad (31)$$

$$A'' = e^{\frac{3}{2}\beta J}[20e^{\beta D}+9][e^{-5\beta J'}+e^{-2\beta J'}+e^{3\beta J'}] \quad (35)$$

$$B'' = 3e^{\frac{3}{2}\beta J}[4e^{\beta D}+1][e^{-5\beta J'}+e^{-2\beta J'}+e^{3\beta J'}] \quad (36)$$

$$C'' = 3e^{-\frac{3}{2}\beta J}[8e^{\beta D}+2]e^{-2\beta J'} \quad (37)$$

On the other hand, the internal magnetic energy per site can be obtained by :

$$U(T,h) = -\frac{\partial ln(Z)}{\partial \beta} \quad (38)$$

while the specific magnetic heat can be derived from $u(T,h)$ as

$$C_m = \frac{\partial U(T,h)}{\partial T} \quad (39)$$

Additionally, the entropy given by

$$S(T,h) = \frac{U-F}{T} \quad (40)$$

where F is the Helmholtz thermodynamic free energy per site $F = -\frac{1}{\beta} lnZ$

With the help of Maxwell's thermodynamic equations, such physical variables can be used to examine the magnetocaloric effect of the molecule. Certain of the above variables are used for magnetic refrigerator characteristics, such as the isothermal change in magnetic entropy:, [12]:

$$\Delta S(T,h) = \int_0^h \left(\frac{\partial S(T,h)}{\partial h}\right)_T dh' = \int_0^h \left(\frac{\partial m(T,h')}{\partial T}\right)_{h'} dh' \quad (41)$$

(since $\left(\frac{\partial S(T,H)}{\partial h}\right)_T = \left(\frac{\partial m}{\partial T}\right)_h$)

We can also use the simple expression of the adiabatic entropy

$\Delta S_{ad}(T,\Delta h) = S(T,h) - S(T,0)$

or the adiabatic temperature given by :

$$\Delta T(T,h) = -\int_0^h \frac{T}{C_m(T,h')} \left(\frac{\partial m(T,h')}{\partial T}\right)_{h'} dh' \quad (43)$$

When the analytical calculations are completed, we can investigate the magnetic and magnetocaloric properties of the molecule.

2. Outcomes and analysis

2.1 Ferromagnetic case: towards a molecular super magnet

Figure 2 (a) depicts isothermal magnetization curves for J= 10K, J'=5K , D=0, and some selected temperatures (T=3, 4 and 5K). In this example, we see that when the exchange couplings are ferromagnetic and sufficiently strong, all the spins can be polarized in the same direction, particularly at low temperatures, resulting in a large spin ground state of S'=4. A comparison of the exactly calculated curve and the Brillouin function for an effective spin 4 is illustrated in Figure 2(b).

Therefore, the cluster can be considered as a molecular super-magnet that could be used to produce a magnetocaloric effect at the nanoscale, or provide various applications especially in nanomedicine, such as highly targeted and non-destructive therapies [13].

The magnetic field created by this dipole, in a volume of radius $r \sim 10\mathring{A}$, can be roughly estimated by $B_d \sim \frac{\mu_0 g\, \mu_B S}{2\pi r^3} \sim 0.15\, Tesla$. This is a huge field compared to the cardiac or cerebral activity fields of about 10^{-11} and 10^{-14} T respectively [9, 14]. Obviously, as nanotechnology advances with smaller devices and structures, there is growing interest in assigning specific functions to such single molecules. Thus, it is quite realistic for us to come up with such innovative proposals for these nanomagnets.

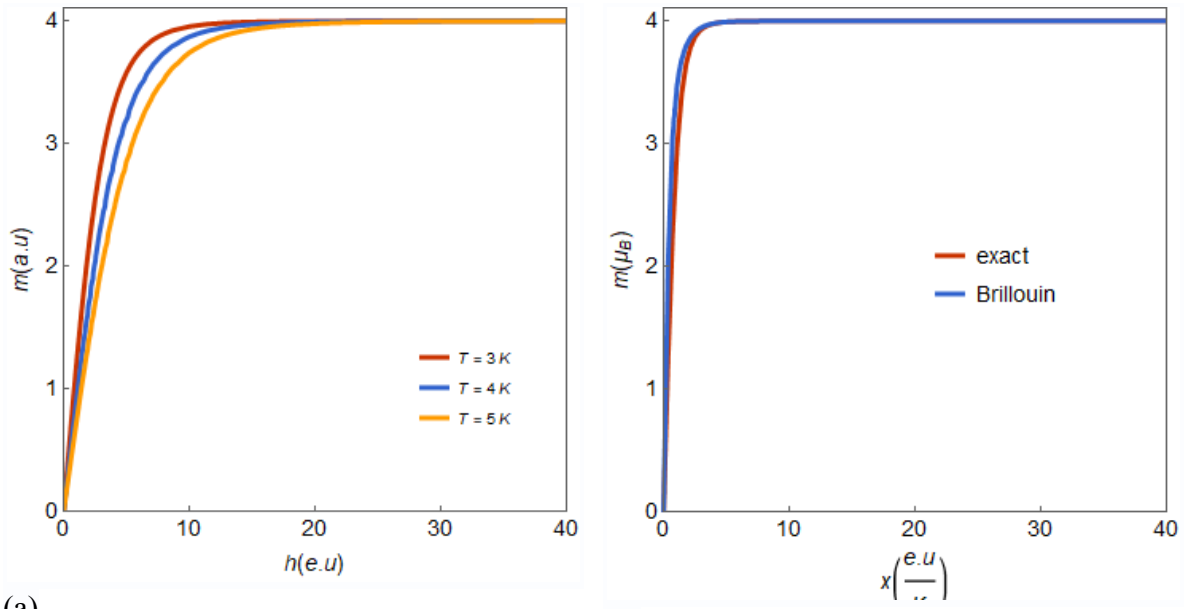

(a) (b)

Figure 2: Magnetization isotherms for J=10K, J'=5K, D=0K, at low temperature (a). Comparison of the exactly calculated curve and the Brillouin function for an effective spin-4 (b).

The initial susceptibility is also displayed in Figure 3, for J=10K, J'=5K, and D=0. It follows a Curie-Weiss law as illustrated by its inverse, reflecting the dominant ferromagnetic correlations among the spins of the molecule.

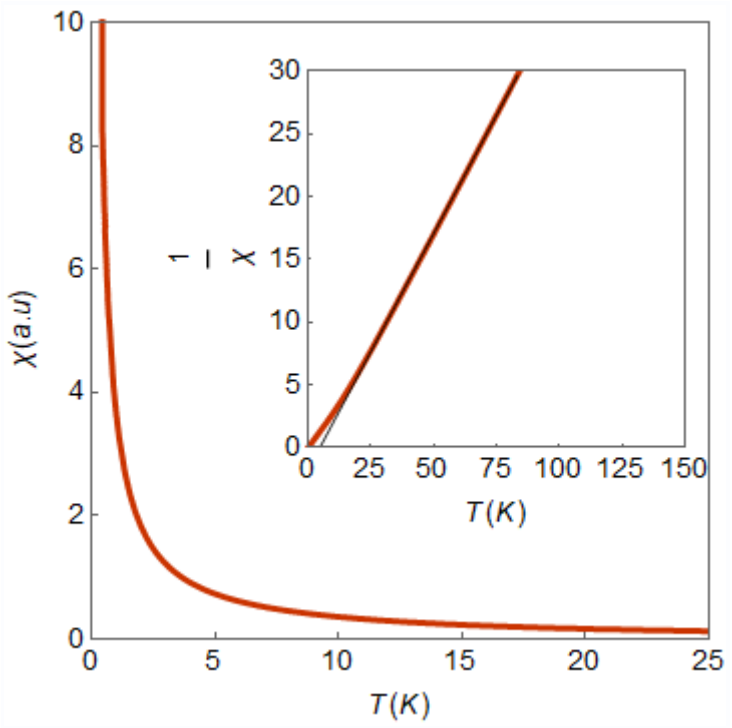

Figure 3: Thermal evolution of the initial magnetic susceptibility for J=10K, J'=5K,and D=0. The insert indicates the reciprocal susceptibility, which intercepts the T-axis at a weakly positive value indicating the ferromagnetic correlation.

The magnetic internal energy evolution with temperature is plotted in Fig. 4, for J=10K, J'=5K, D=0, and a set of selected applied fields (h = 0-10 e.u). At low temperatures, all the spins are aligned with the effective field and the internal energy is close to $-\ g\mu_B SB_{eff}$, where B_{eff} stands for the sum of the applied and the internal (due to exchange) fields. At T=0, |U(T=0)| increases with applied field since the field strengthens correlations among spins, and further stabilizes their ferromagnetic configurations within the cluster. As U(T) increases with temperature, it exhibits an inflexion point where both the exchange and the applied field, working for spin-spin correlations, are overcomed by thermal agitation. As T gets very large, the energy tends to zero as the spins become completely disoriented.

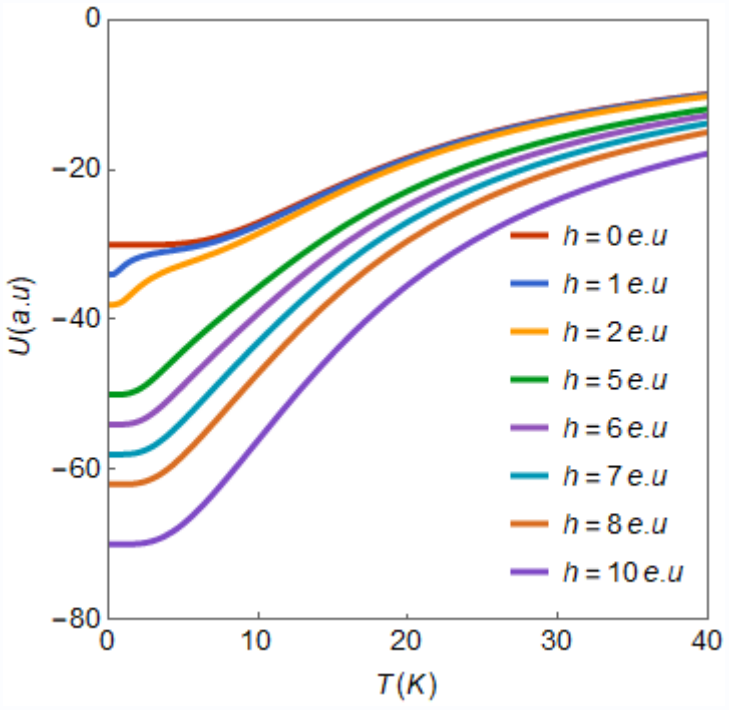

Figure 4: The magnetic internal energy evolution with temperature for J=10K, J'=5K D=0, and some values of the applied field (h=0-10 e.u).

The magnetic specific heat C_m relates changes in the system's temperature T to changes in its magnetic internal energy density ($dU=C_m dT$), and can be used to shed light on excitations. The magnetic specific heat evolution with temperature is depicted in Figure 5, for J=10K, J'=5K, and D=0, and a set of applied fields (*h* =0 - 10 *e.u*). There is a broad peak resulting from correlations through the spins of the molecule, while the curves decay exponentially below the peak, and in the thermodynamic limit, $C_m(T)$ tends to 0. This peak separates two phases: a correlated phase and a high-temperature decorrelated phase which arises when thermal agitation overrides the exchange couplings. The heat capacity is small at low temperatures because the thermal fluctuations that cause spins to flip are very rare, and it is difficult for the system to absorb heat.

In a low magnetic field, the heat capacity shows a familiar round peak owing to the short-range ferromagnetic correlations and a small Schottky peak developed in low-temperature region [15].

The magnetic specific heat displays in zero field a broad Shottky peak typical of low dimensional and small correlated systems, separating a correlated phase at low temperature and a fully paramagnetic phase at high temperature. It can also be seen that in low fields, a sharper peak appears at low temperature, then it moves to join the broad peak as the applied field is increased [15].

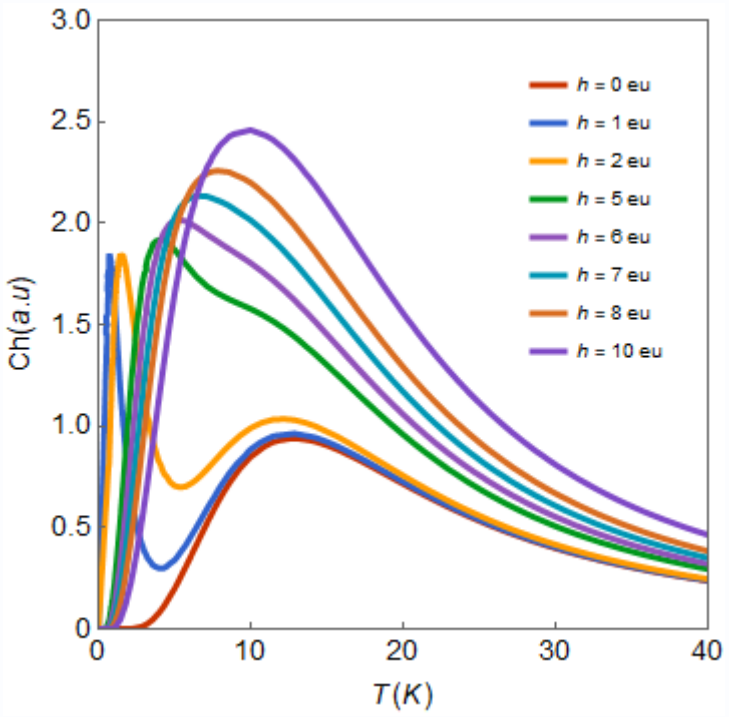

Figure 5 :Thermal evolution of the magnetic specific heat for J=10K, J'=5K; D=0K, and some selected values of the applied field (h = 0 -10 e.u).

The thermal variation of the magnetic entropy is plotted in Figure 6 for J=10K, J'=5K, D=0, and a set of applied fields (h=0-10 e.u.). The entropy increases progressively with temperature, exhibits an inflection point before reaching an asymptotic limit value at high temperature where the system becomes completely disordered under the thermal agitation influence, and all configurations are equally likely : ($S(T)_{T\to\infty} \to 2Ln(2S' + 1) = 2Ln(9) = 4.39$). Similar behavior was observed in polyoxovanadate molecular magnet V6 containing 6 vanadium ions carrying quantum spins S= ½ [16].

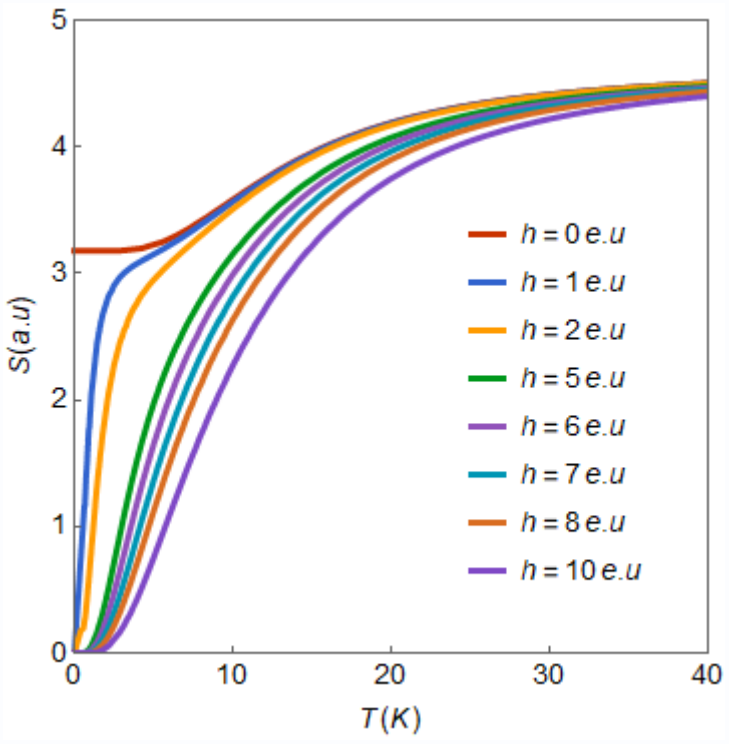

Figure 6 : Evolution of the magnetic entropy with temperature for J=10K, J'=5K; D=0K, and some selected values of the applied field (h = 0 -10 e.u).

Figure 7 illustrates the isothermal entropy change $-\Delta S(T, h)$ for several fields. It can be seen that $-\Delta S$ is asymmetric since the system does not display a finite critical temperature. Besides, the width of $-\Delta S$ increases with the applied field. Localized magnetic refrigeration at low temperature could be considered with such a molecule. Similar features have been revealed in V6 molecular magnet [16].

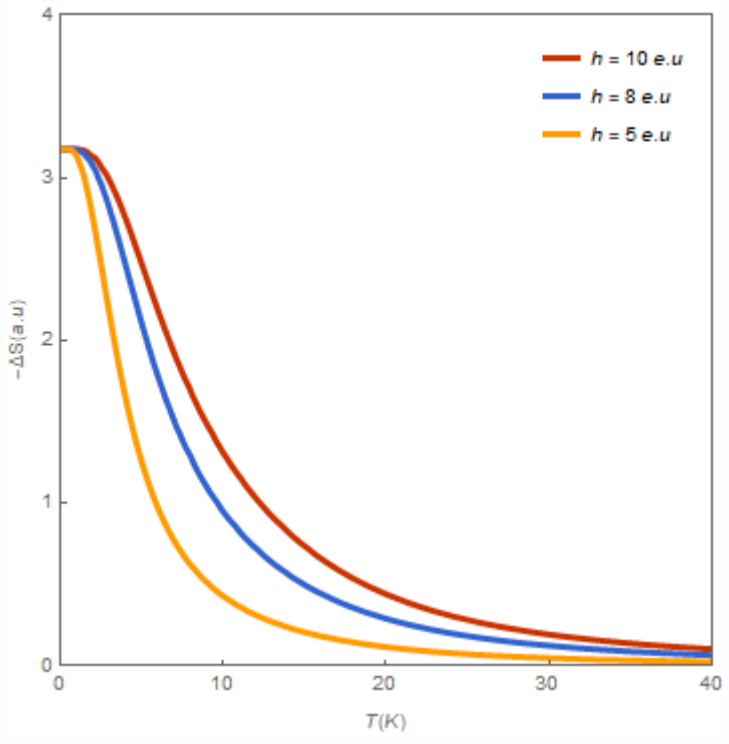

Figure 7 : The magnetic entropy change vs temperature for J=10K, J'=5K; D=0K, and some selected values of the applied field (h = 0 -10 e.u).

2.2 Competitive couplings : magnetization plateaus and molecular ferrimagnetism

Our discussion here is focused on conflictual ferro/antiferromagnetic couplings that are characterized by many novel phenomena.

Fig. 8 shows a set of isothermal magnetizations for |J|=10K, |J'|=5K and D=0 at several low temperatures. We note that the magnetization exhibits a plateau at half of its saturation value, up to a critical field h_{c1} where it abruptly goes into saturation. Throughout an intermediate plateau, the magnetization remains constant, the system takes on several different states of the same magnetization, before switching to another plateau: the system thereby displays a gap separating the groups of states. In a previous work, we have revealed such a type of magnetization plateaus in a single tetrahedral molecule with spin ½ [17].

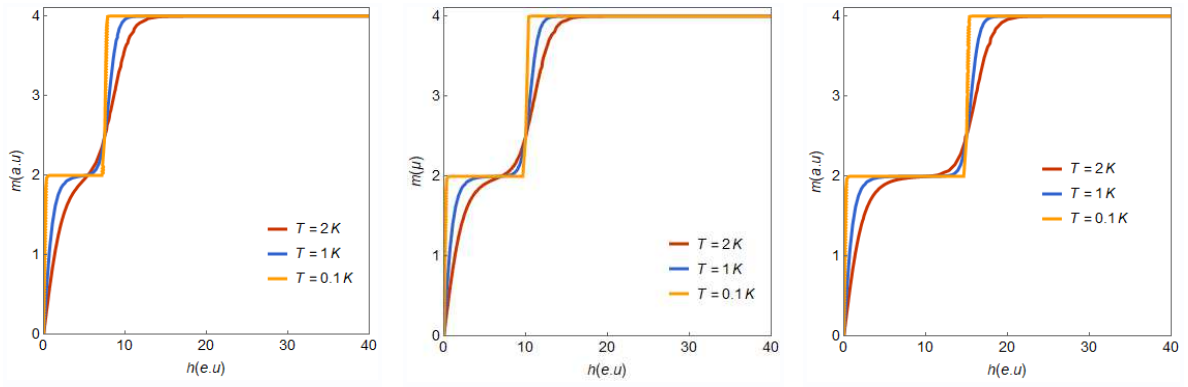

(a) J=10K et J'=-5K **(b) J=-10K, J'=5K** **(c) J=-10K et J'=-5K**

Fig. 8 : Isothermal magnetization vs the applied field for J=10K, J'=-5K (a), J=-10K, J'=5K (b) and J=-10K, J'=-5K (c) at several low temperatures.

The magnetization switching field h_{c1} depends on the value and sign of the exchange parameters (J, J'). From Figures 8 (a, b, c), corresponding to (J=10K, J'=-5K), (J=-10K, J'=-5K) and (J=-10K, J'=-5K), it is evident that the magnetization exhibits an intermediate plateau at the same $M_s/2$ value since the exchange ratio is the same J'/J=½, while the plateau's width grows with frustration.

Indeed, in curve a, the magnetization saturates at h_{c1}=7e.u, while in Figs. 8(b) and (c) it saturates at h_{c1}=12e.u, and h_{c1}=16 e. u. respectively. The interpretation is simple: in case (a), the spins inside each triangle are ferromagnetically correlated to one other but antiferromagnetically correlated to the central spin. As a result, h_{c1} corresponds in this case to the field where the central spin goes to the S_z=+1 state. Since the spins of each triangle exchange antiferromagnetically in case (b), the frustrated state is more pronounced, delaying

the switch to saturation at a higher field than in case (a). In case (c), both the triangle's spins and the center spin are in the AF state, so the frustration is even greater. This leads to a higher switching field than in the two previous cases. Such plateaus could be used to implement magnetic regulators or filters [18]. Ferrimagnetic structures combine the advantages of both ferromagnets and antiferromagnets, such as the ability to detect the net magnetization with an external field, their antiferromagnetic-like dynamics faster than ferromagnet dynamics, and their potential for creating high-density devices [19].

The entropy behavior provides useful information when correlated with other thermal quantities. As shown in Figure 9, the entropy versus temperature is plotted for J=-10K, J'=5K, and D=0 for different applied fields. The curves in this figure are monotonically increasing with temperature. Such monotonous behavior is indicative of a stable physical system. However, some residual entropy remains for $T \rightarrow 0$. The residual entropy indicates that the ground state is degenerate.

In the tetrahedron, since its basic triangles contain three antiferromagnetic spins, each spin can take on several configurations without impacting the global magnetization, which explains both the residual entropy due to degeneracy as well as the appearance of plateaus in the magnetization curves (Fig.8).

Since the central spin is antiferromagnetically coupled to the six spins of the two tetrahedra bases, these spins have different configuration possibilities without changing the total magnetization, which explains on the one hand the degeneracy, and on the other hand, the magnetization plateaus (Fig.8).

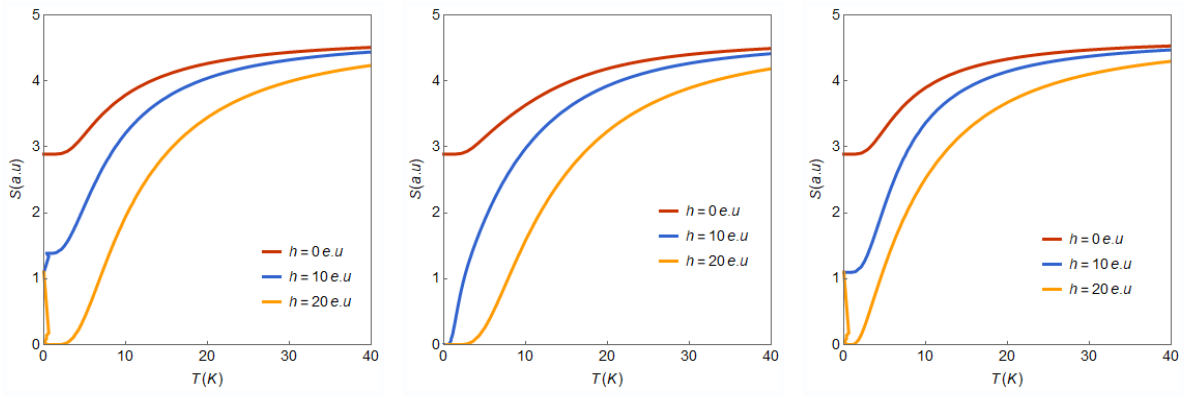

a) J=-10K,J'=5K,D=0K b) J=10K,J'=-5K,D=0K c) J=-10K,J'=-5K,D=0K

Figure 9: Entropy versus temperature for J=-10K, J'=5K, D=0 (a); J=10K, J'=-5K, D=0 (b) ; and J=-10K, J'==5K, D=0 (c), for different applied fields.

Due to their unique characteristics, molecular-scale ferrimagnets are expected to improve the tunability of functional spintronic devices, such as spin reorientation or non-collinear magnetic states. In this regard, miniaturization is crucial in order to achieve ultra-high bit densities. These disruptive technologies present fundamental challenges both for fabricating

these magnetic nanostructures as well as controlling the magnetic properties of ferrimagnets in reduced dimensions [19].

Conclusion

In this work, we have studied the magnetic and thermodynamic properties of a double tetrahedral molecule of spin-½ which is coupled to another atom of spin-1 via exchange coupling at their common summit.

When ferromagnetic coupling occurs among the spins, the cluster behaves as a giant pseudo-spin with a value of S=4, which may be used to generate large spin ground states, revealing many phenomena like residual entropy at zero fields and shotky's peak of specific heat at low temperatures.

In the presence of competing ferro/antiferromagnetic exchange couplings, several exotic phenomena have been observed as a result of the frustration governing the spin edifice. By solving the eigenvalue equations with the isotropic Heisenberg model, we demonstrated that frustration creates quantized magnetization plateaus. The transition from one plateau to the other is purely quantum.

Our results should pave the way for single-molecular magnets and their potential device applications.

References

[1] Puxian Xiong | Chibin Zheng | Mingying Peng | Zhihao Zhou | Feifei Xu | Kexin Qin | Yiyu Hong | Zhijun Ma , *Self-activated persistent luminescence from Ba2Zr2Si3O12 for information storage*, Journal of the American Ceram Soc. 2020;00:1–10, DOI: 10.1111/jace.17412

[2]Atsufumi Hirohata, Keisuke Yamada, Yoshinobu Nakatani, Ioan-Lucian Prejbeanu, Bernard Diény, Philipp Pirro, Burkard Hillebrands, *Review On Spintronics: Principles Device Applications*, Journal of Magnetism and Magnetic Materials 509 (2020)166711, DOI:10.1016/j.jmmm.2020.166711

[3] Claudio Puglia,Giorgio De Simoni, and Francesco Giazotto,*Gate Control of Superconductivity in Mesoscopic All-Metallic Devices,*Materials 2021, 14, 1243. https://doi.org/10.3390/ma14051243.

[4]Boisseau P, Loubaton B (2011). "*Nanomedicine, nanotechnology in medicine*". Comptes Rendus Physique. **12** (7) (2011) 620–636. Bibcode:2011CRPhy..12..620B. doi:10.1016/j.crhy.2011.06.001.

[5] Berry CC, Curtis AS "*Functionalization of magnetic nanoparticles for applications in biomedicine*". *J. Phys. D*. **36** (13) (2003): R198. Bibcode:2003JPhD...36R.198B. doi:10.1088/0022-3727/36/13/203. S2CID 16125089
[6] Qin, Lei and Zhang, Hao-Lan and Zhai, Yuan-Qi and Nojiri, Hiroyuki and Schröder, Christian and Zheng, Yan-Zhen, *A Giant Spin Molecule with Ninety-Six Parallel Unpaired Electrons* (October 13, 2020). Available at SSRN: https://ssrn.com/abstract=3710312 or http://dx.doi.org/10.2139/ssrn.3710312
[7]Xuanhe Zhao & Yoonho Kim*, Soft microrobots programmed by nanomagnets,* Nature 575, 58-59 (2019)
[8] J.U. Reveles, P.A. Clayborne, A.C. Reber, S.N. Khanna, K. Pradhan, P. Sen, M.R. Pederson, *Designer magnetic superatoms*, Nat. Chem. 1 (2009) 310–315.
[9]*Magnétisme : I-Fondements*, sous la direction d'Etienne du Trémolet de Lacheisserie, Préface Louis Néel, EDP Sciences 2000, page 263, ISBN 2868834639

[10] Thorsten Glaser, Maik Heidemeier,Thomas Weyhermüller, Rolf-Dieter Hoffmann, Holger Rupp, Paul Müller, *Property-Oriented Rational Design of Single-Molecule Magnets: A C3-Symmetric Mn6Cr Complex based on Three Molecular Building Blocks with a Spin Ground State of St=21/2*, **Angew. Chem. Int. Ed. 36/2006,** Volume 45, Issue36, September 11, 2006, Pages 6033-6037, https://doi.org/10.1002/anie.200600712,

[11]Andreas Helmstedt , Norbert Muller , Aaron Gryzia, Niklas Dohmeier , Armin Brechling, Marc D Sacher , Ulrich Heinzmann , Veronika Hoeke, Erich Krickemeyer, Thorsten Glaser, Samuel Bouvron, Mikhail Fonin and Manfred Neumann , *Spin resolved photoelectron spectroscopy of [Mn~IICrIII]3+ single-molecule magnets and of manganese compounds as reference layers,* Journal of Physics : Condensed Matter 23 (2011) 26, 266001
[12] A.M. Tishin, Y.I. Spichkin, The Magnetocaloric Effect and Its Applications (Institute of Physics Publishing, Bristol, 2003)
[13] Veronica Clavijo-Jordan, Vikram D. Kodibagkar, Scott C. Beeman, Bradley D. Hann and Kevin M. Bennett, *Principles and emerging applications of nanomagnetic materials in medicine*, Wiley Interdisciplinary Reviews Nanomedicine and Nanobiotechnology 4(4) (2012):345-65, DOI: 10.1002/wnan.1169
[14] Pei-Feng Lin, Men-Tzung Lo, Jenho Tsao, Yi-Chung Chang, Chen Lin, and Yi-Lwun Ho , *Correlations between the Signal Complexity of Cerebral and Cardiac Electrical Activity: A Multiscale Entropy Analysis*, PLoS One. 2014; 9(2): e87798, 2014, doi: 10.1371/journal.pone.0087798
[15] Saeed Mahdavifar and Alireza Akbari , Heat capacity of Schottky type in low-dimensional spin system, *J. Phys.: Condens. Matter*, Vol. 20 (2008) 215213, DOI: 10.1088/0953-8984/20/21/215213

[16] P. Kowalewska and K. Szałowski, *Magnetocaloric properties of V6 molecular magnet*, Journal of Magnetism and Magnetic Materials, Volume 496, 15 February 2020, 165933, https://doi.org/10.1016/j.jmmm.2019.165933.

[17] Said IdBakas and Mohamed El Hafidi, *Frustration effect and possibility of spin quantum liquid state in a tetrahedral spin ½ molecule*, Chinese Journal of Physics, Volume 73, October 2021, Pages 433-441, https://doi.org/10.1016/j.cjph.2021.07.005

[18] M.A.G.Soler, and L.G.Paterno, *Magnetic Nanomaterials*, Nanostructures,2017, 147-186,https://doi.org/10.1016/B978-0-323-49782-4.00006-1
[19]Kim, S.K., Beach, G.S.D., Lee, KJ. et al., *Ferrimagnetic spintronics.* Nat. Mater. 21, 24–34 (2022). https://doi.org/10.1038/s41563-021-01139-4